EIC Physics Note: Longitudinal Nucleon Spin Structure Inclusive and Semi-Inclusive Reactions to Access Quark Helicity Distribution

Notes on Kinematic, Statistic Uncertainties and Physics Impacts

Xiaodong Jiang, Los Alamos National Laboratory

06/23/2013

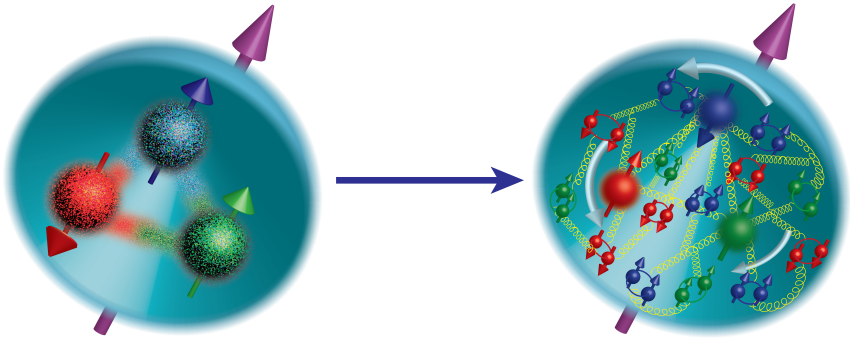

Pe=3 GeV * Pp=12 GeV

root_s=12.04 GeV
Ee0_fixed_target_equiv=76.85 GeV, roughly half of COMPASS-II beam energy.

COMPASS-II muon beam on fixed target p_mu=160 GeV.

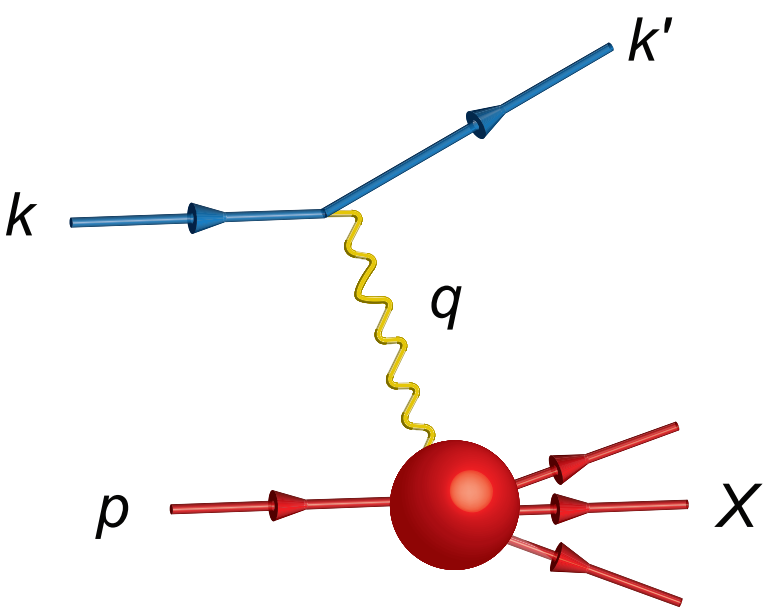

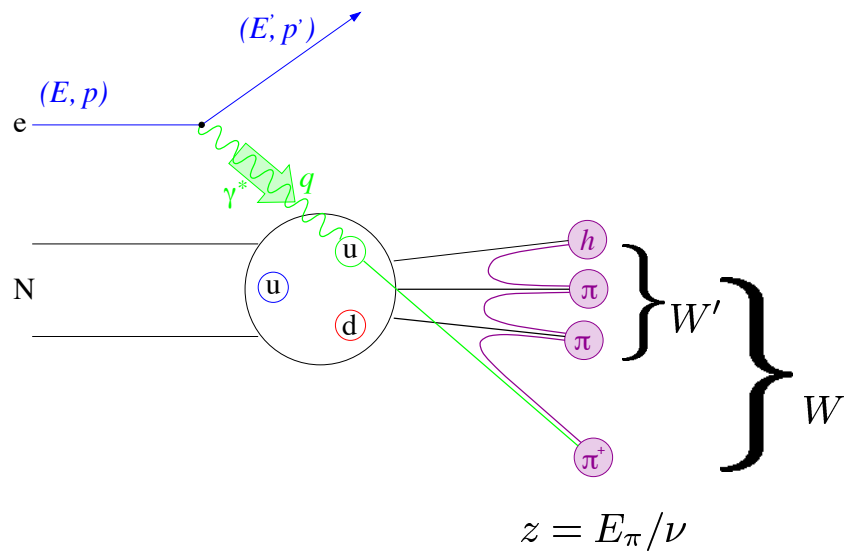

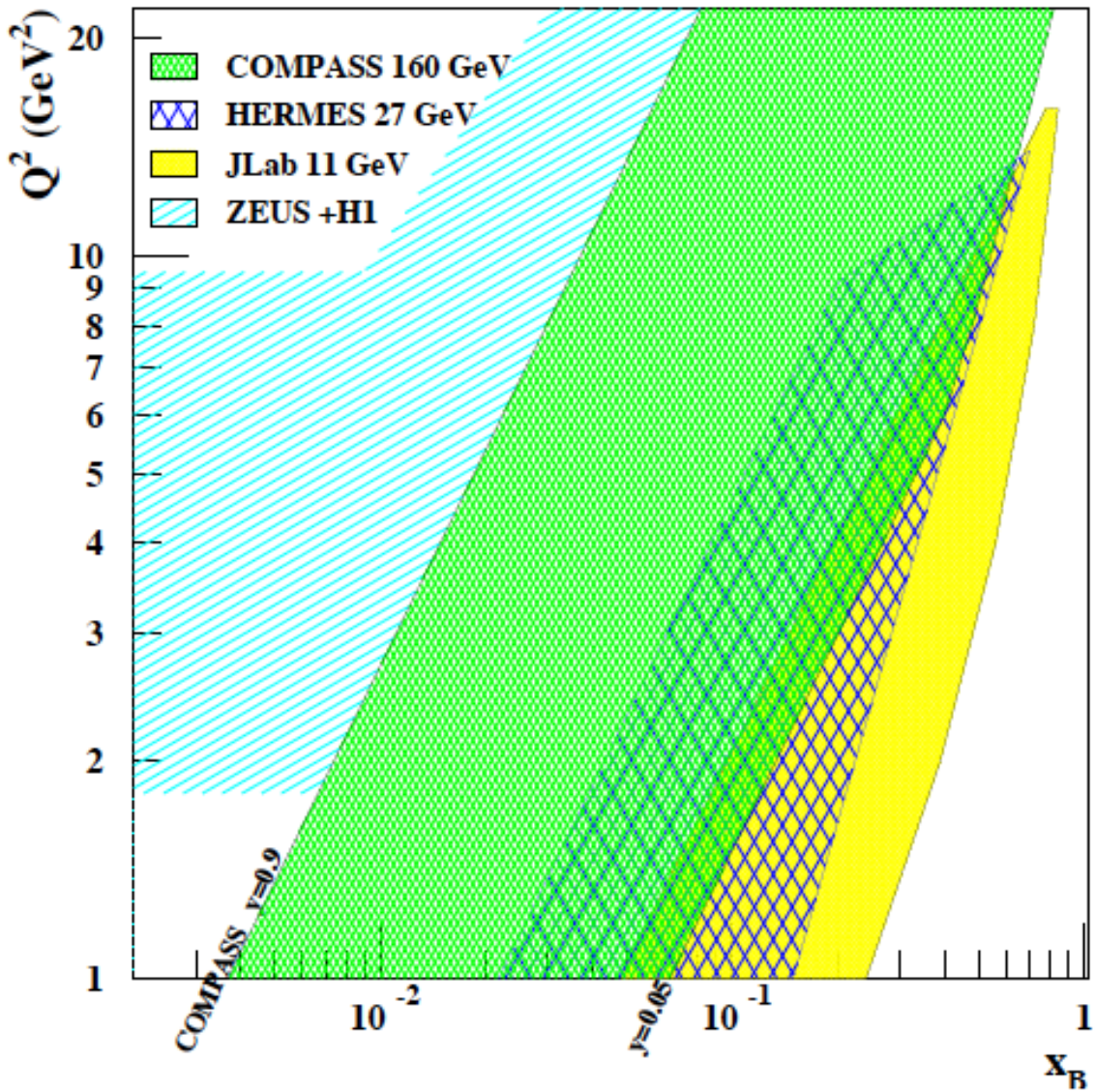

Figure 3: Kinematic domains for measurements of hard exclusive processes shown for the COMPASS (green area enclosed by the lines $y = 0.9$ and $y = 0.05$), HERMES and JLAB fixed-target experiments and the HERA collider experiments H1 and ZEUS. COMPASS will explore the uncharted territory in between the collider region and that of the lower-energy fixed-target HERMES and JLAB experiments.

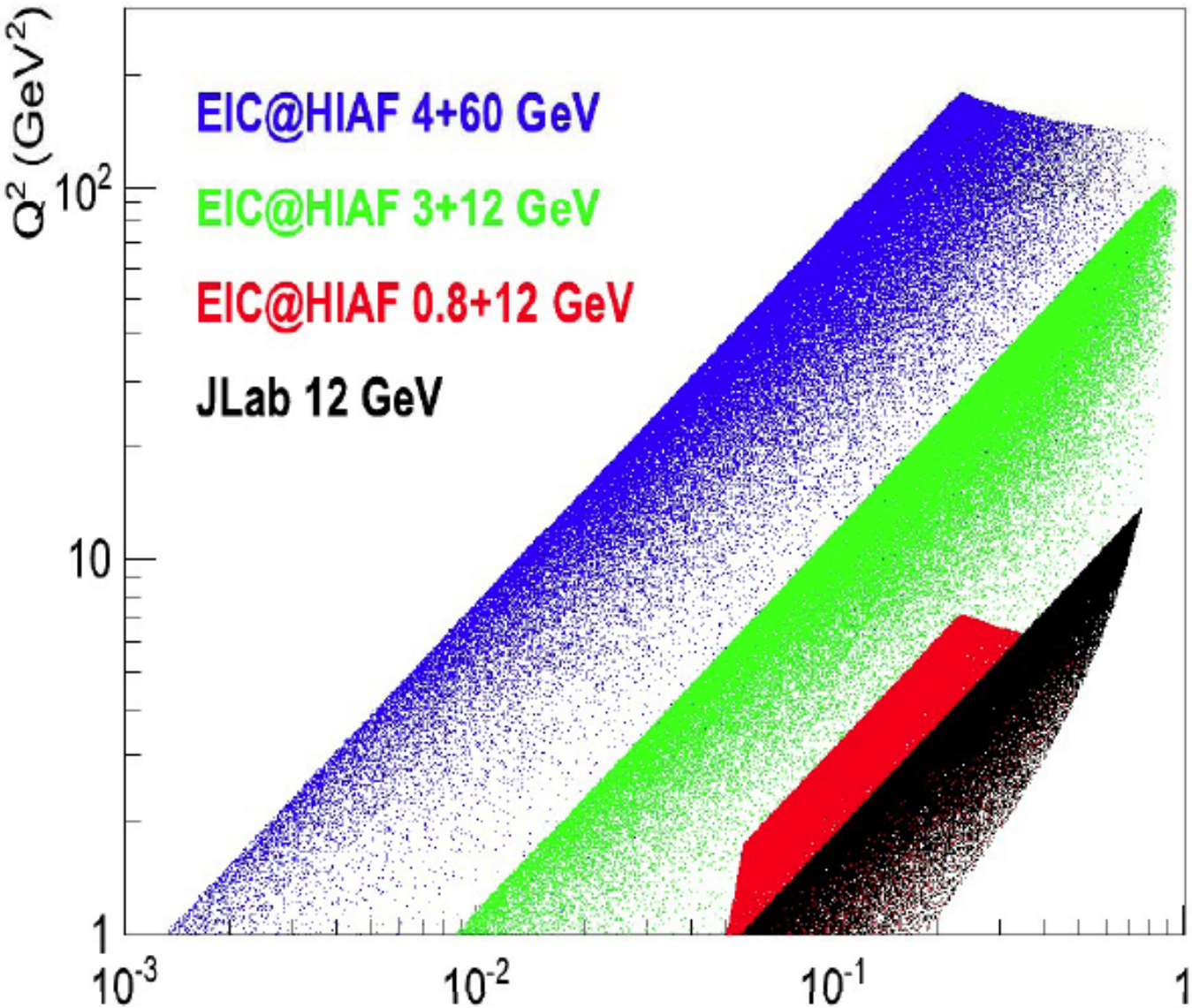

Dr. Xurong Chen, Lanzhou Meeting, April 1st, 2013.

Following the COMPASS-2010 paper: charm quarks not included in \Delta q analysis

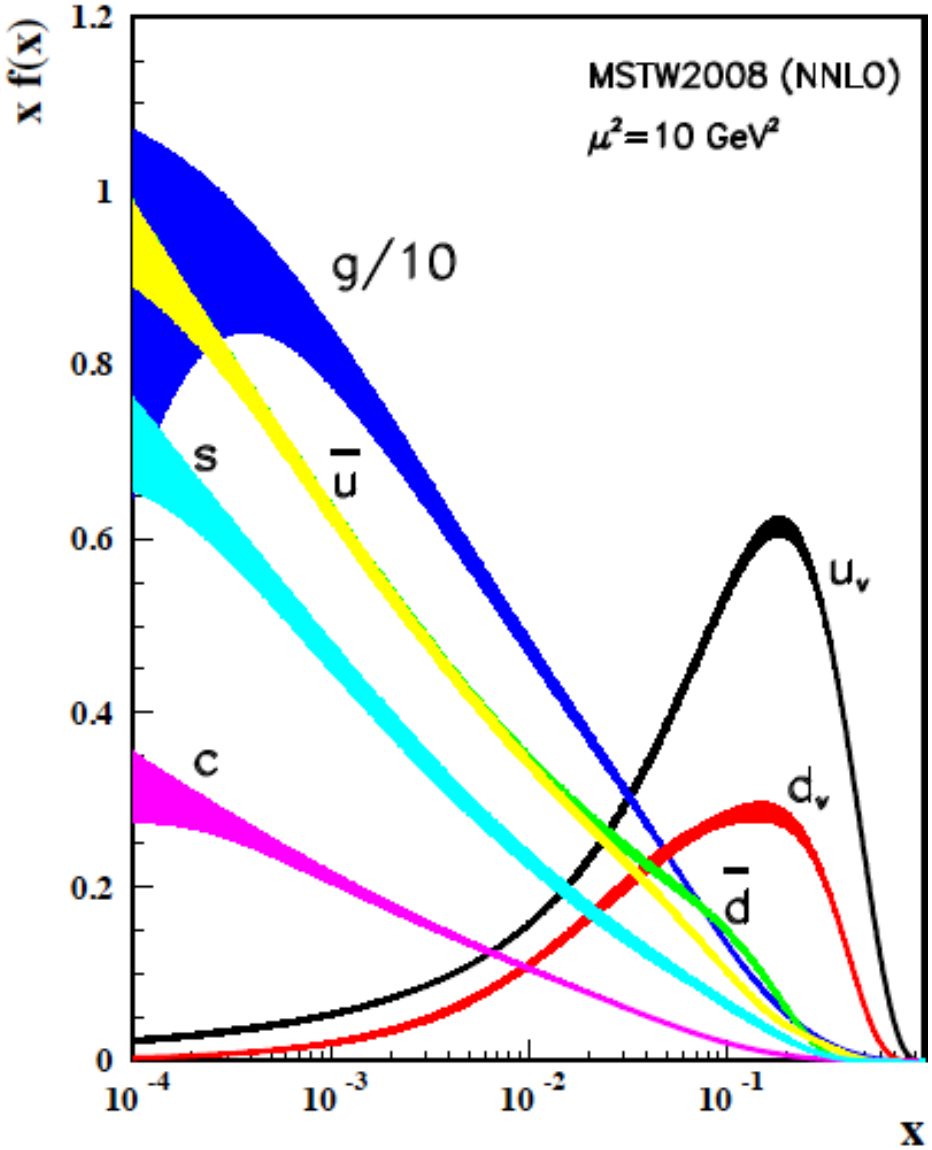

Charm quark contributions can be not negligible at x=0.01-0.1 and Q2>3.0. We include charm quark terms in total DIS cross sections, but not in SIDIS \Delta-q studies.

Also note that COMPASS 2010 paper did not include charge contributions.

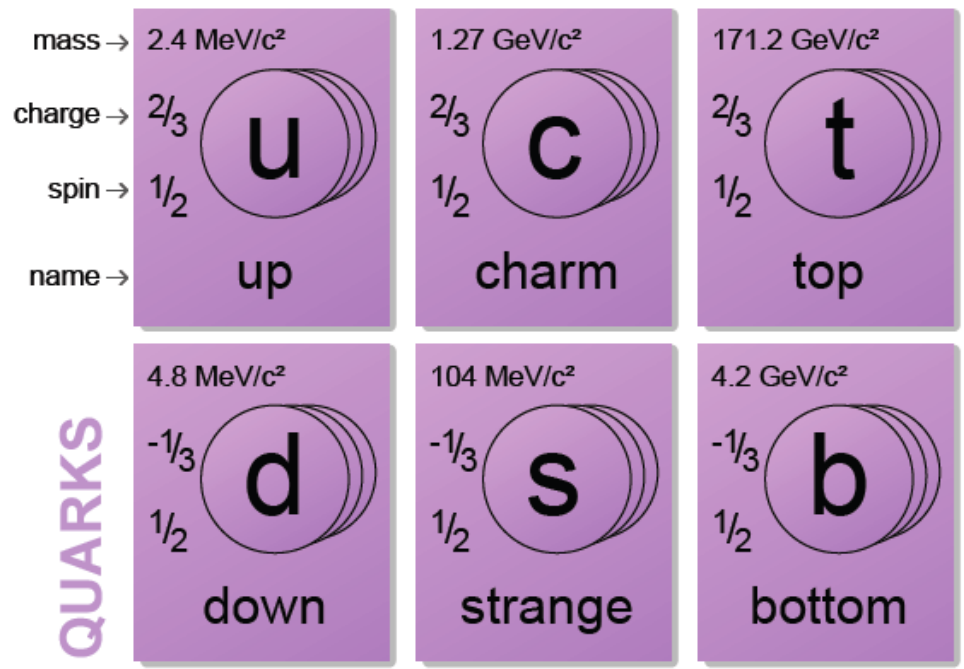

Intend to update this plot.

Existing Data on g1p

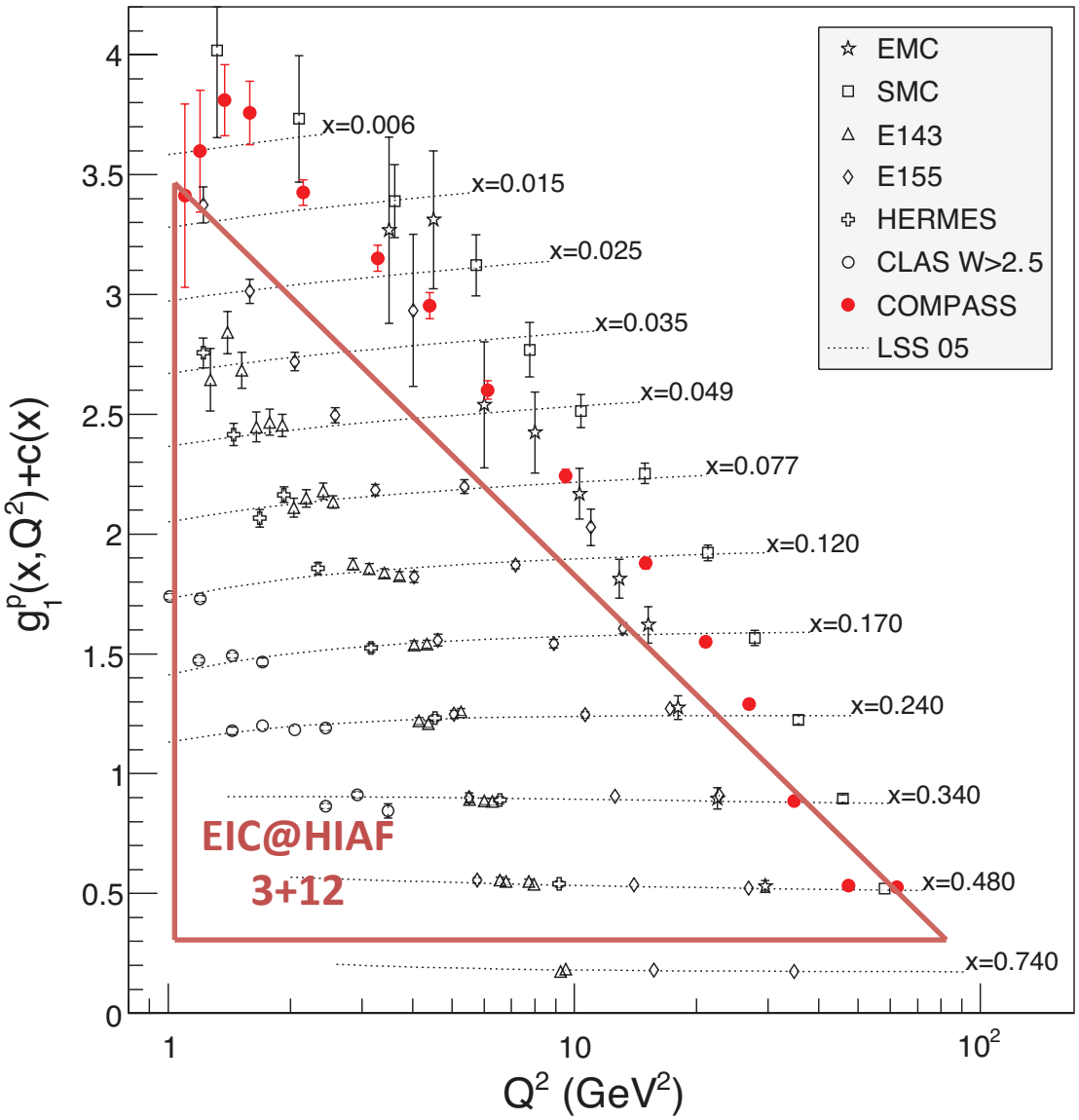

COMPASS paper
PLB693,227,2010

Intend to update this plot.

EIC White Paper

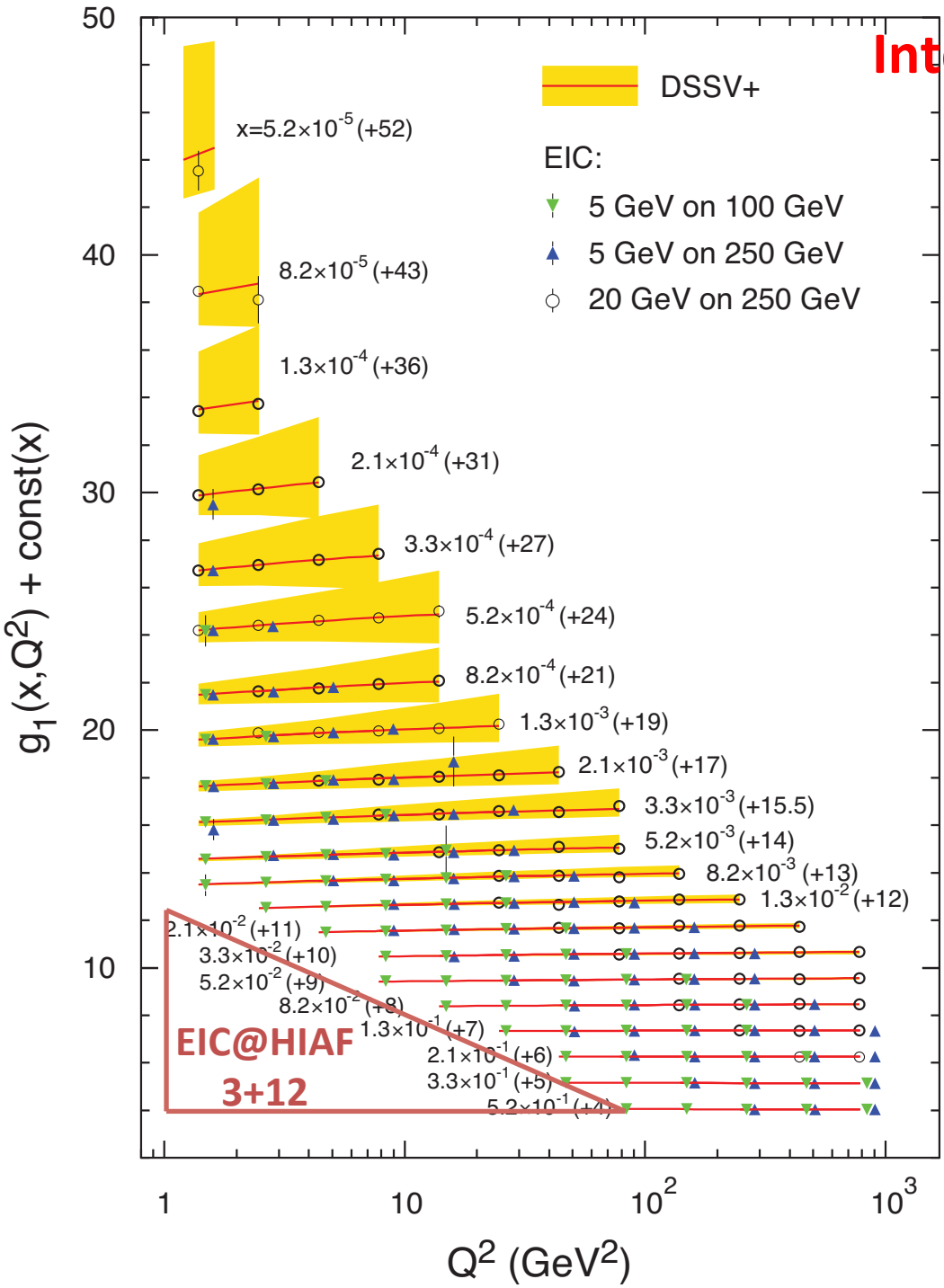

Intend to update this plot.

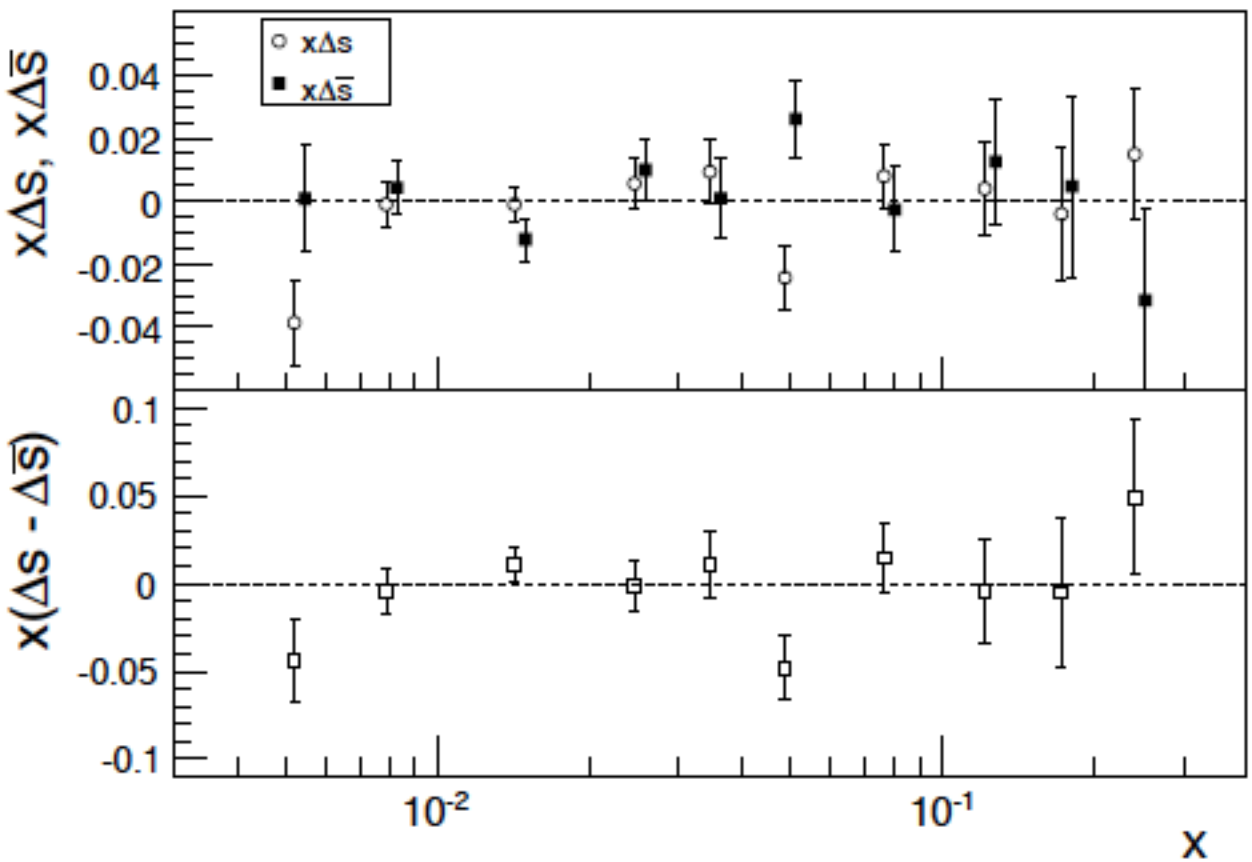

Fig. 2: Comparison of $x\Delta s$ (open circles) and $x\Delta\bar{s}$ (squares) at $Q_0^2 = 3$ (GeV/c)^2 (top) and corresponding values of the difference $x(\Delta s - \Delta\bar{s})$ (bottom).

COMPASS paper
PLB693,227,2010

Intend to update this plot.

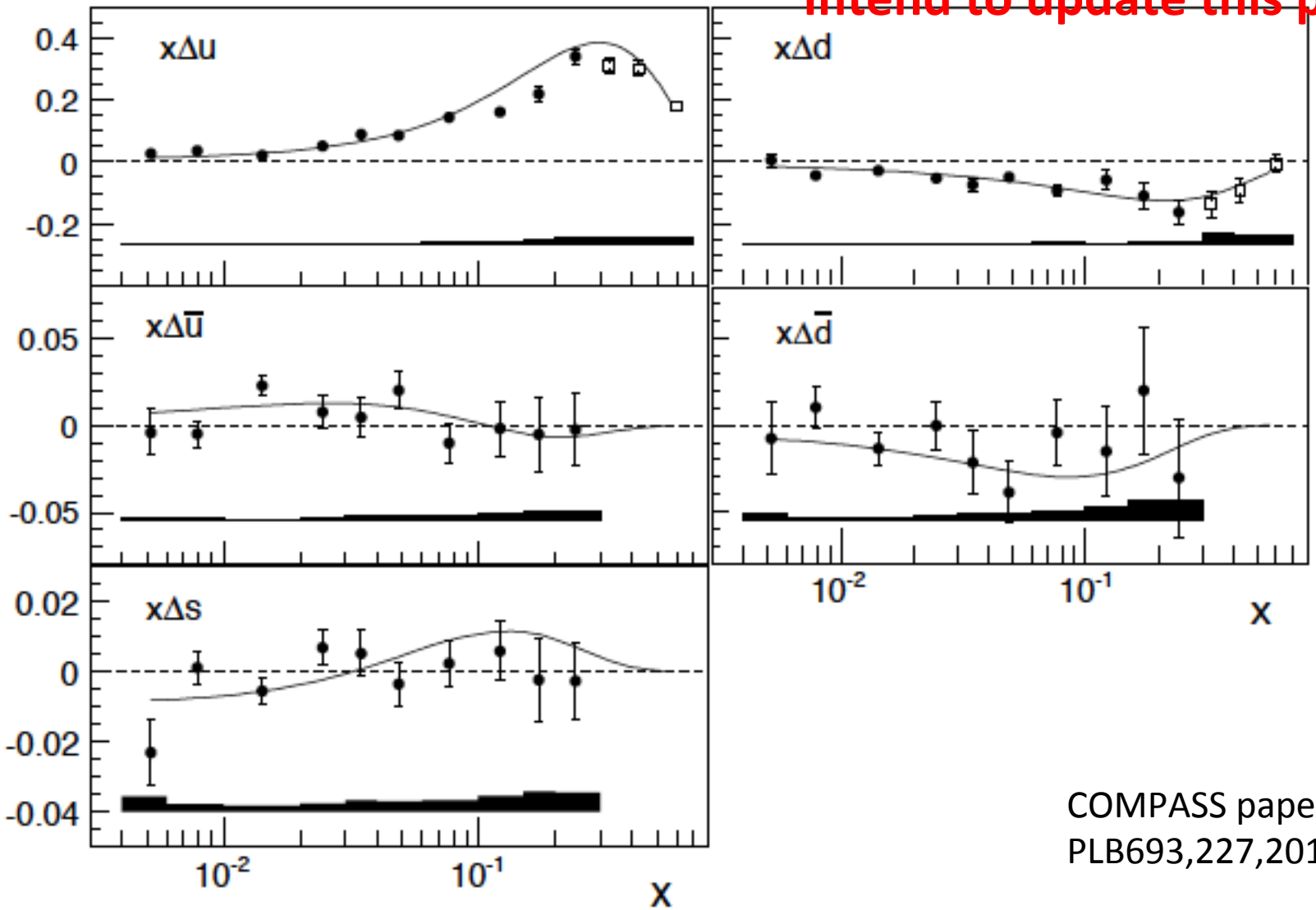

COMPASS paper
PLB693,227,2010

Fig. 3: The quark helicity distributions $x\Delta u$, $x\Delta d$, $x\Delta\overline{u}$, $x\Delta\overline{d}$ and $x\Delta s$ at $Q_0^2 = 3$ (GeV/c)^2 as a function of x. The values for $x < 0.3$ (black dots) are derived at LO from the COMPASS spin asymmetries using the DSS fragmentation functions [30]. Those at $x > 0.3$ (open squares) are derived from the values of the polarised structure function $g_1(x)$ quoted in [20,35] assuming $\Delta\overline{q} = 0$. The bands at the bottom of each plot show the systematic errors. The curves show the predictions of the DSSV fit calculated at NLO [1].

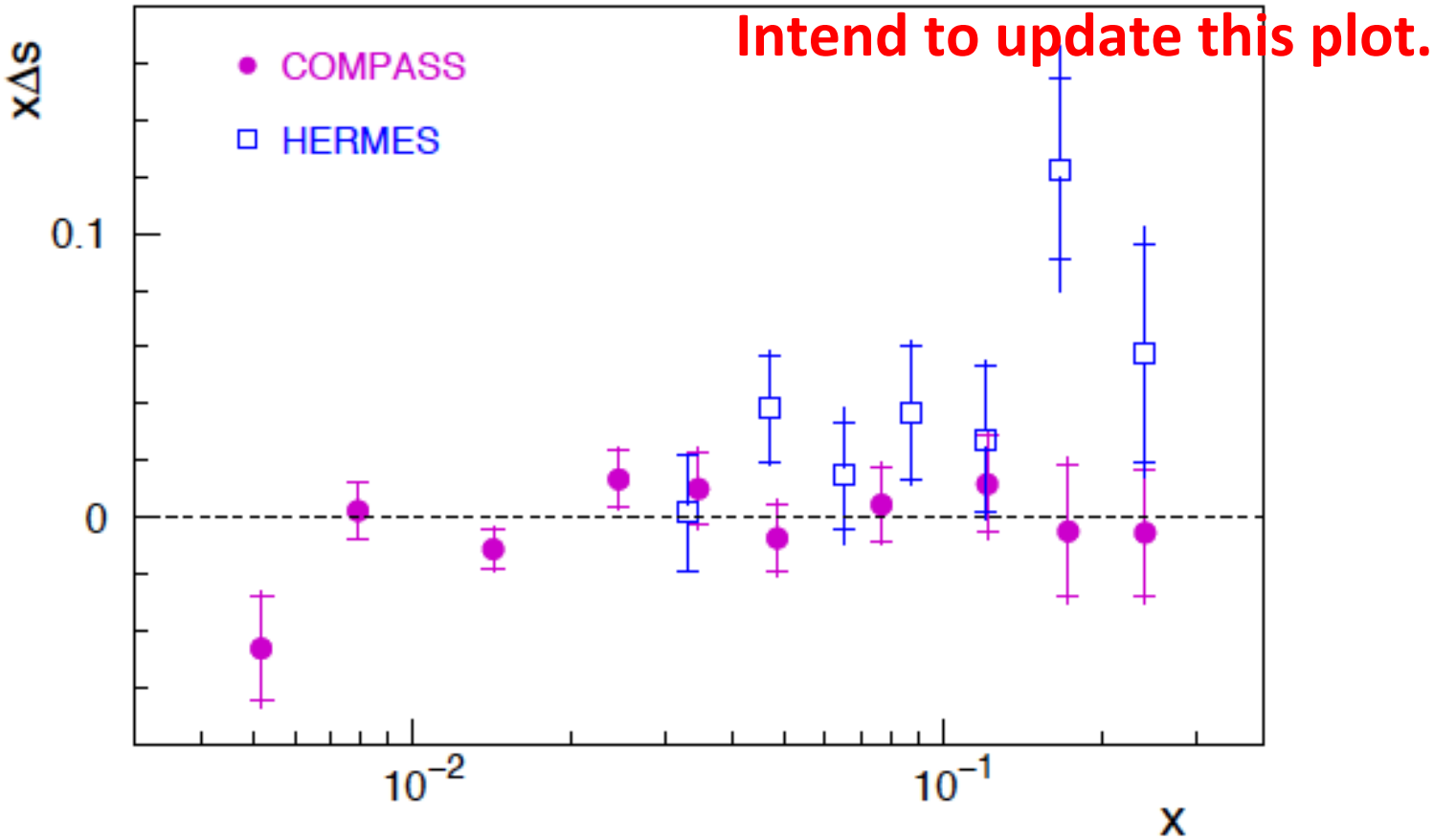

FIG. 8 COMPASS (Alekseev *et al.*, 2010c) and HERMES (Airapetian *et al.*, 2008c) results for the strangeness polarization $x\Delta s(x)$ as function of x. The data are obtained in a leading-order analysis of SIDIS asymmetries (including those for charged kaons) and using the DSS fragmentation functions (de Florian *et al.*, 2007). The inner error bar represents the statistical uncertainty; the full bar the quadratic sum of statistical and systematic uncertainties.

Intend to update this plot.

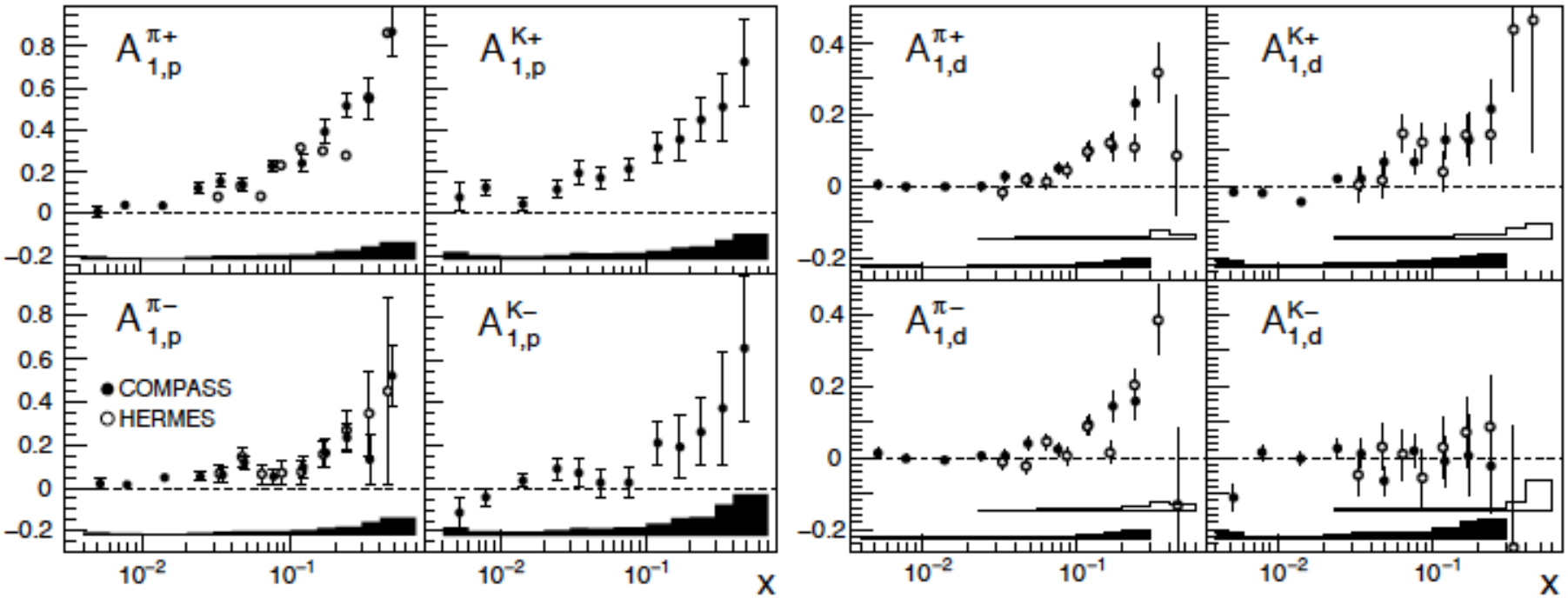

FIG. 7 Semi-inclusive longitudinal double-spin asymmetries for identified pions and kaons from COMPASS (Alekseev *et al.*, 2009b, 2010c) and HERMES (Airapetian *et al.*, 2005a) for the proton (left) and the deuteron (right) as function of x at the Q^2 of the measurements. The error bars and bands indicate the statistical and systematic uncertainties, respectively. Figure adapted from Alekseev *et al.* (2009b) (left, proton target) and Alekseev *et al.* (2010c) (right, deuteron target).

COMPASS paper
PLB693,227,2010

Intend to update this plot.

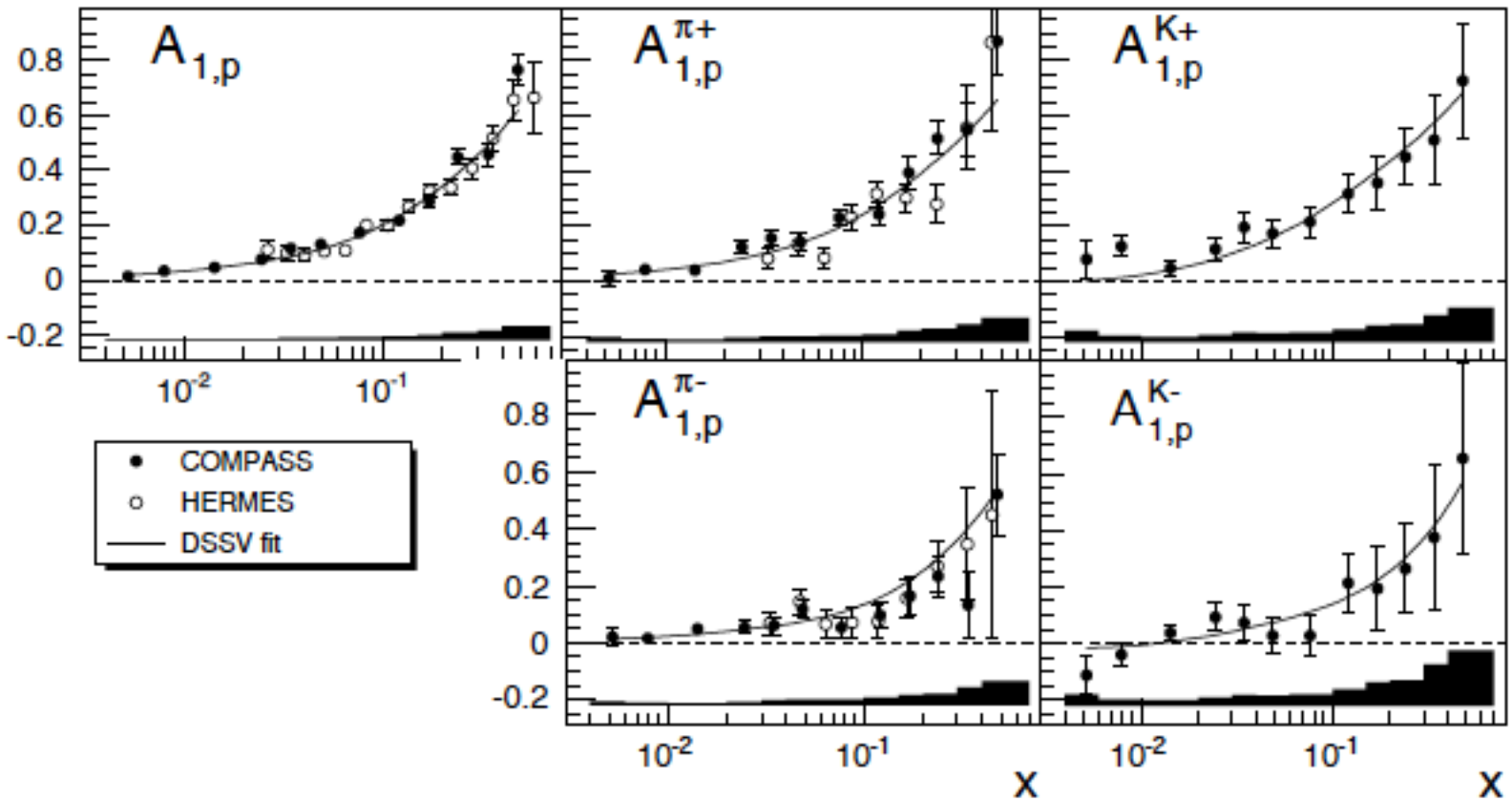

Fig. 1: The inclusive asymmetry $A_{1,p}$ [20] and the semi-inclusive asymmetries $A^{\pi+}_{1,p}$, $A^{K+}_{1,p}$, $A^{\pi-}_{1,p}$, $A^{K-}_{1,p}$ from the present measurements (closed circles). The bands at the bottom of each plot show the systematic errors. The $A_{1,p}$, $A^{\pi+}_{1,p}$ and $A^{\pi-}_{1,p}$ measurements from HERMES [14, 26] (open circles) are shown for comparison. The curves show the predictions of the DSSV fit [1].

Intend to update this plot.

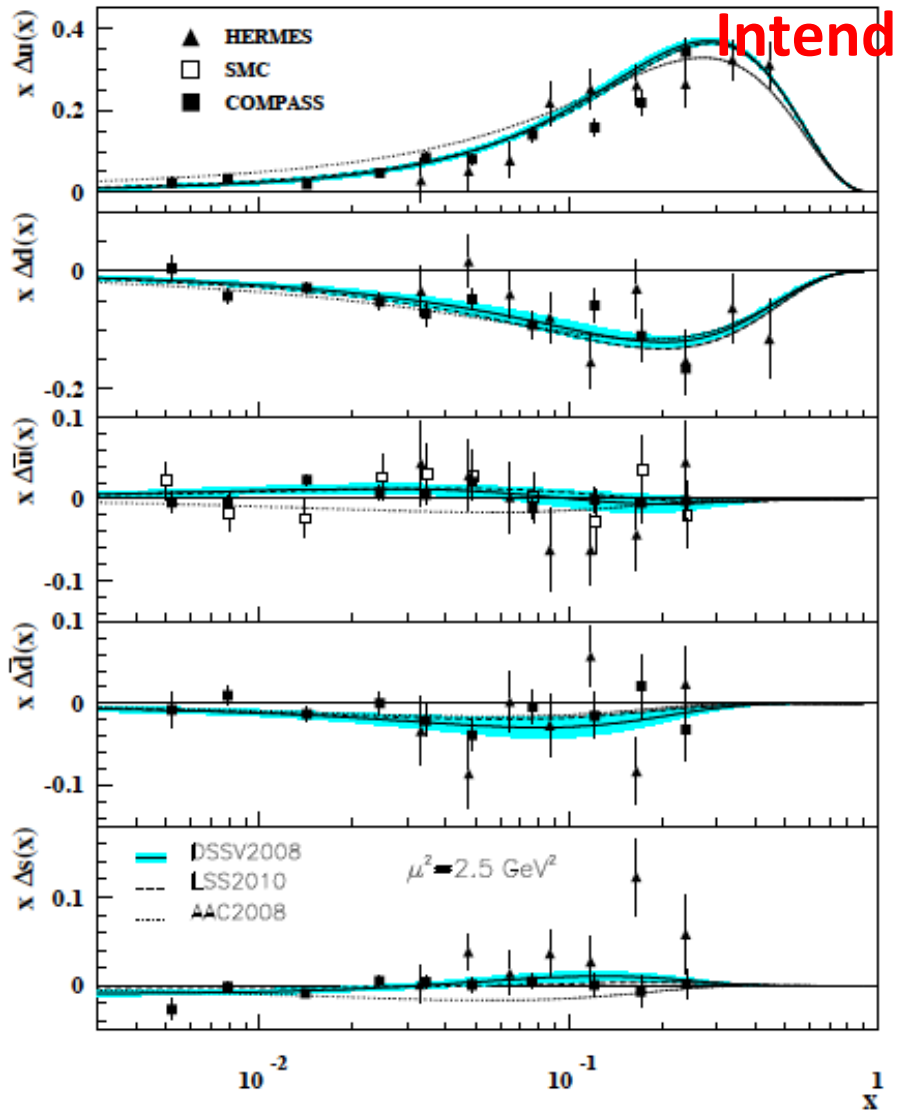

Figure 16.5: Distributions of x times the polarized parton distributions $\Delta q(x)$ (where $q = u, d, \overline{u}, \overline{d}, s$) using the LSS2010 [57], AAC2008 [54], and DSSV2008 [55] parameterizations at a scale $\mu^2 = 2.5$ GeV^2, showing the error corridor of the latter set (corresponding to a one-unit increase in χ^2). See also BB2010 [56]. Points represent data from semi-inclusive positron (HERMES [61,62]) and muon (SMC [63] and COMPASS [64,65]) deep inelastic scattering given at $Q^2 = 2.5$ GeV^2. SMC results are extracted under the assumption that $\Delta\overline{u}(x) = \Delta\overline{d}(x)$.

Intend to update this plot.

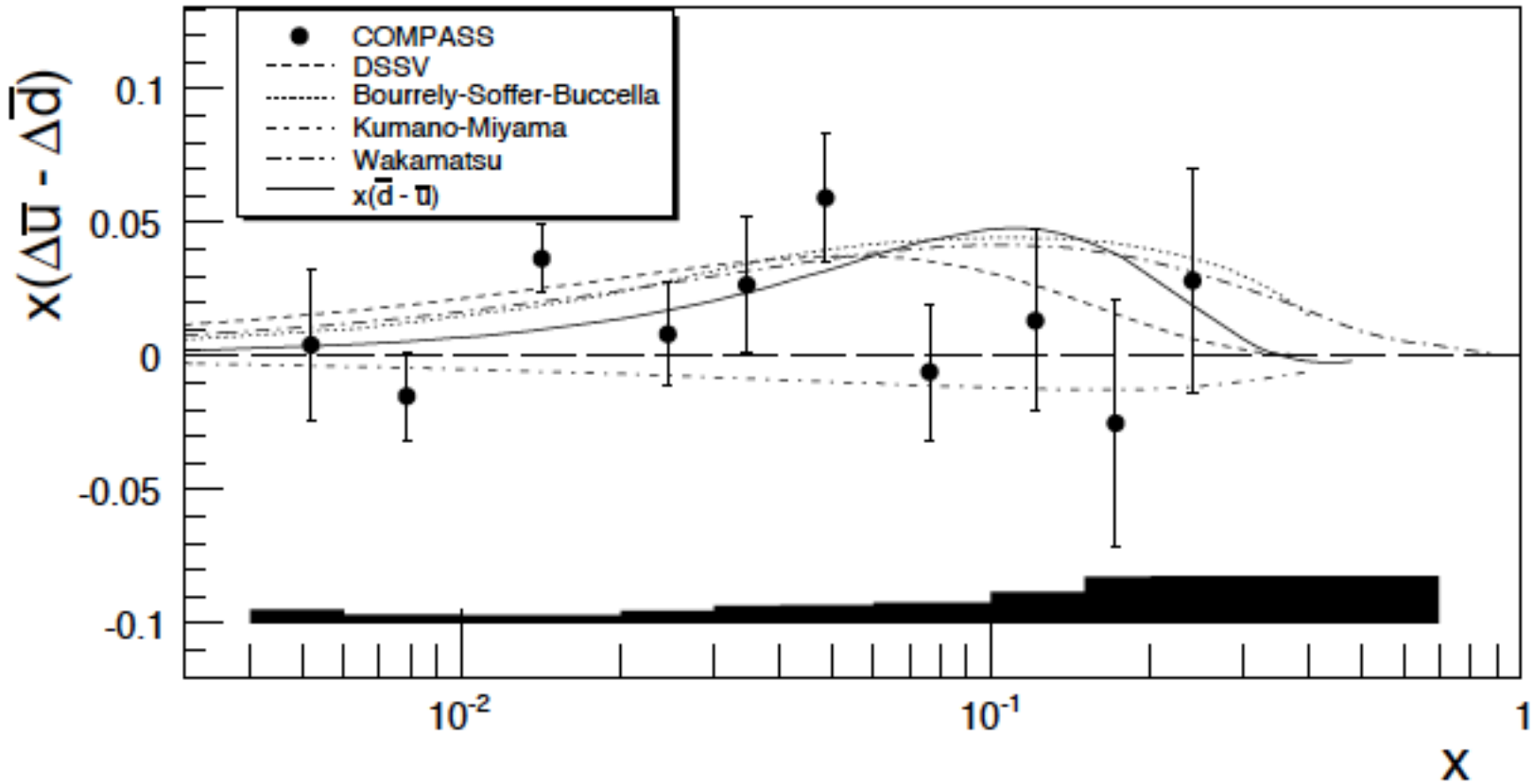

Fig. 4: The flavour asymmetry of the helicity distribution of the sea $x(\Delta\overline{u} - \Delta\overline{d})$ at $Q_0^2 = 3\ (\mathrm{GeV}/c)^2$. The shaded area displays the systematic error. The dashed curve is the result of the DSSV fit at NLO. The other curves are model predictions from Wakamatsu [33] (long dash-dotted line), Kumano and Miyama [39] (short dash-dotted line) and Bourrely, Soffer and Buccella [10] (dotted line). The solid curve shows the MRST parameterisation for the unpolarised difference $x(\overline{d} - \overline{u})$ at NLO.

COMPASS paper
PLB693,227,2010

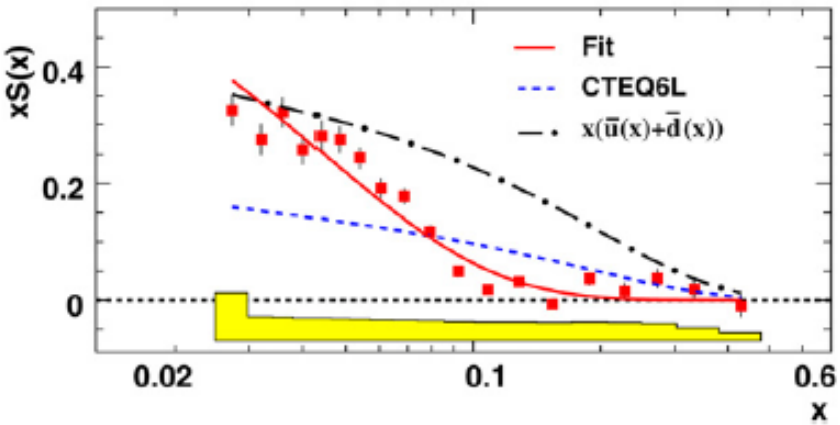

Fig. 3. The strange parton distribution $xS(x)$ from the measured HERMES multiplicity for charged kaons evolved to $Q_0^2 = 2.5$ GeV^2 assuming $\int \mathcal{D}_S^K(z)\,dz = 1.27 \pm 0.13$. The solid curve is a 3-parameter fit for $S(x) = x^{-0.924} e^{-x/0.0404}(1-x)$, the dashed curve gives $xS(x)$ from CTEQ6L, and the dot–dash curve is the sum of light antiquarks from CTEQ6L.

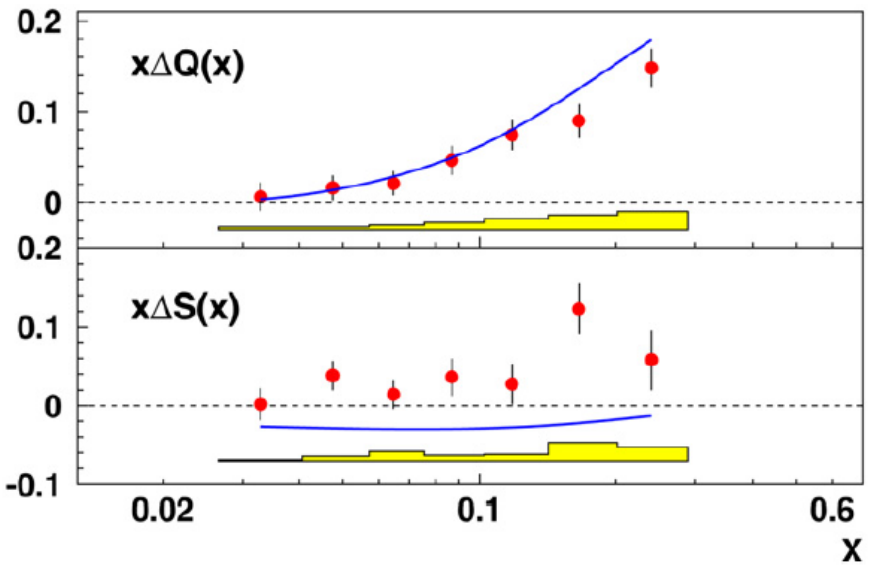

Fig. 5. Nonstrange and strange quark helicity distributions at $Q_0^2 = 2.5$ GeV^2, as a function of Bjorken x. The error bars are statistical, and the bands at the bottom represent the systematic uncertainties. The curves are the LO results of Leader et al. [39] from their analysis of world data.

Intend to update this plot.

HERMES PLB666, (2008)446

$$A_{\text{meas}} = p_B p_T f_D A_{\parallel}$$

$$A_{\parallel} = D(1 + \eta\gamma)A_1$$

where $\eta \equiv \epsilon\gamma y/[1 - (1 - y)\epsilon]$ is a kinematic factor, and $g_2 \approx 0$ is assumed. The factor D depends on x and Q^2, and accounts for the degree of polarization transfer from the lepton to the virtual photon. It is called the depolarization factor and is given by

$$D = \frac{1 - (1 - y)\epsilon}{1 + \epsilon R}, \tag{14}$$

where ϵ is the polarization parameter of the virtual photon,

$$\epsilon = \left[1 + \frac{2\vec{q}^2}{Q^2}\tan^2\frac{\theta}{2}\right]^{-1} = \frac{1 - y - \frac{1}{4}\gamma^2 y^2}{1 - y + \frac{1}{4}y^2(\gamma^2 + 2)}. \tag{15}$$

The photon-nucleon asymmetry A_1 is related to the structure function g_1 by

$$A_1 = \frac{g_1}{F_1}, \tag{16}$$

when $g_2 = 0$. This approximation is justified in view of the

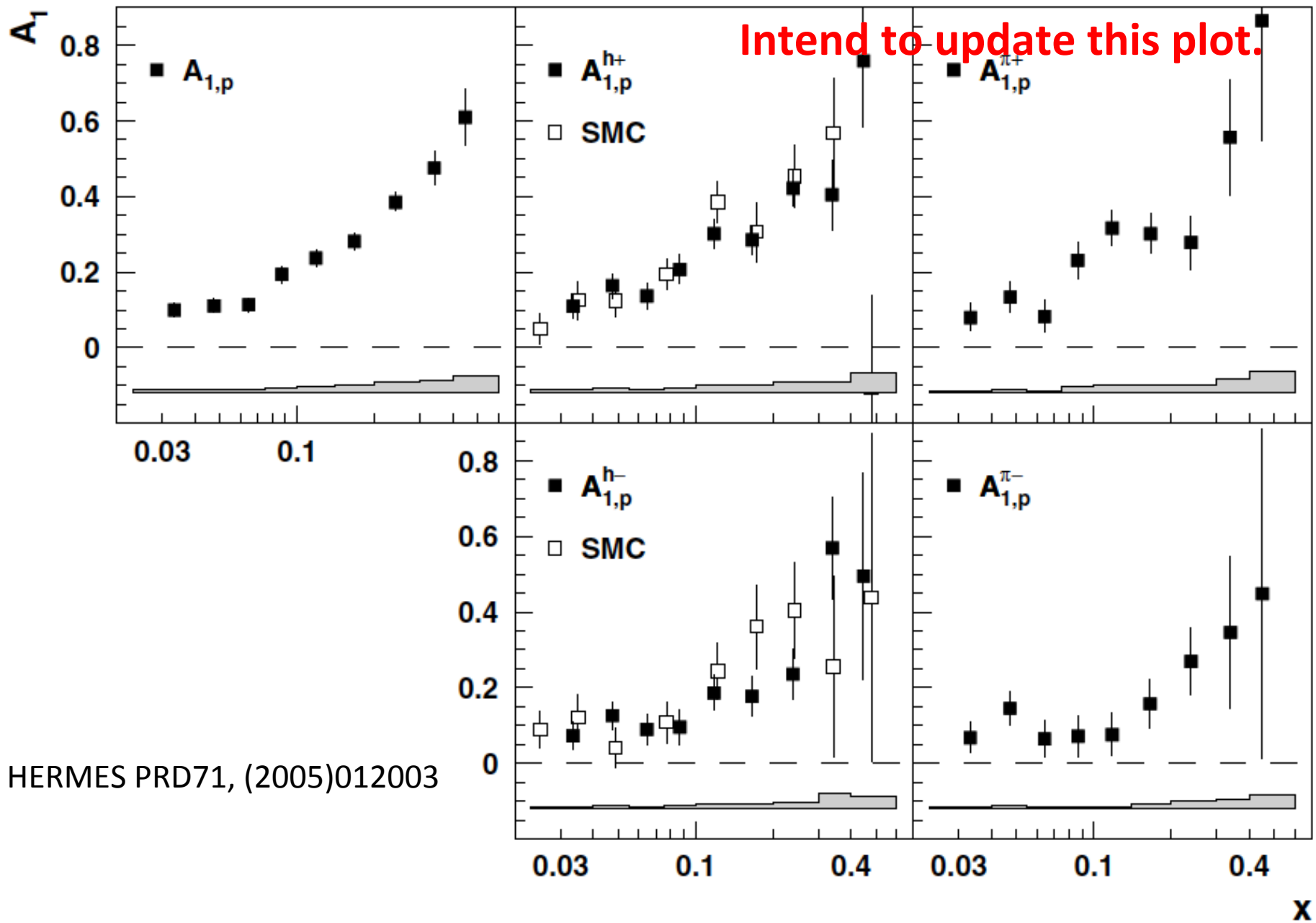

HERMES PRD71, (2005)012003

FIG. 13. The inclusive and semi-inclusive Born level asymmetries on the proton, corrected for instrumental smearing and QED radiative effects. The error bars give the statistical uncertainties, and the shaded bands indicate the systematic uncertainty. The open squares show the positive and negative hadron asymmetries measured by the SMC collaboration, limited to the HERMES x range [50].

$\langle x \rangle$	$\langle Q^2 \rangle / \mathrm{GeV}^2$	$\langle z \rangle$	$A_{1,p}^{\pi^+}$	$\pm$stat	$\pm$syst	$\pm$MC	$A_{1,p}^{\pi^-}$	$\pm$stat	$\pm$syst	$\pm$MC
0.033	1.22	0.364	0.0800	0.0353	0.0058	0.0077	0.0675	0.0388	0.0053	0.0081
0.047	1.50	0.416	0.1336	0.0387	0.0091	0.0088	0.1450	0.0431	0.0095	0.0092
0.064	1.87	0.449	0.0829	0.0408	0.0067	0.0093	0.0649	0.0461	0.0039	0.0100
0.087	2.38	0.471	0.2312	0.0459	0.0157	0.0102	0.0714	0.0536	0.0047	0.0109
0.118	3.08	0.487	0.3163	0.0458	0.0212	0.0093	0.0754	0.0547	0.0057	0.0101
0.166	4.22	0.490	0.3017	0.0525	0.0201	0.0090	0.1572	0.0645	0.0105	0.0102
0.238	5.83	0.504	0.2784	0.0695	0.0197	0.0092	0.2696	0.0889	0.0187	0.0108
0.337	7.97	0.506	0.5566	0.1530	0.0373	0.0138	0.3461	0.1995	0.0233	0.0177
0.449	10.49	0.496	0.8651	0.3185	0.0558	0.0175	0.4490	0.4343	0.0352	0.0270

HERMES PRD71, (2005)012003

Intend to update this plot.

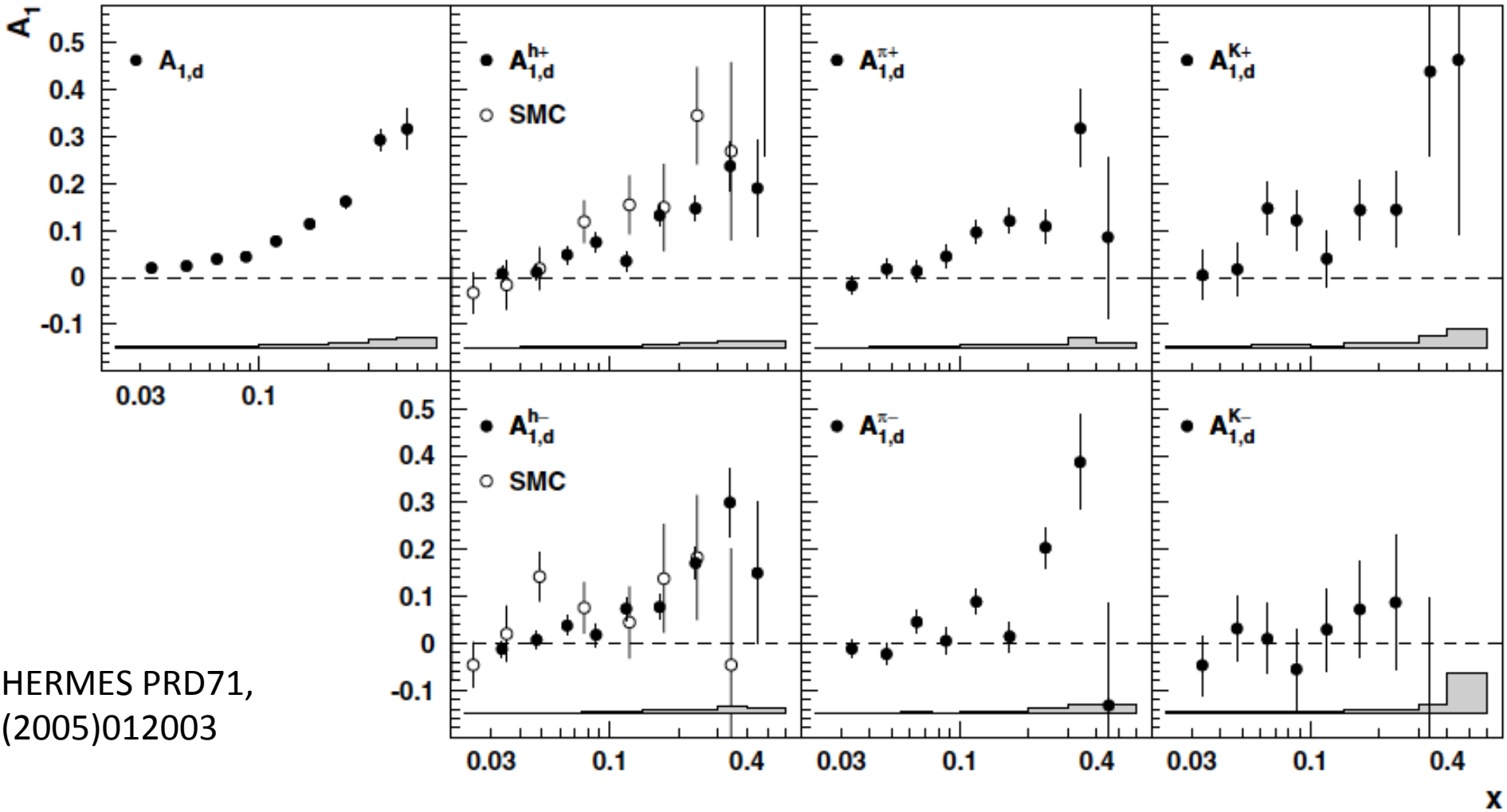

HERMES PRD71, (2005)012003

FIG. 14. The inclusive and semi-inclusive Born level asymmetries on the deuteron. One data point at $x = 0.45$ for the K^- asymmetry including its large error bar is outside the displayed range; all data points are listed in Table XIII. See Fig. 13 for details.

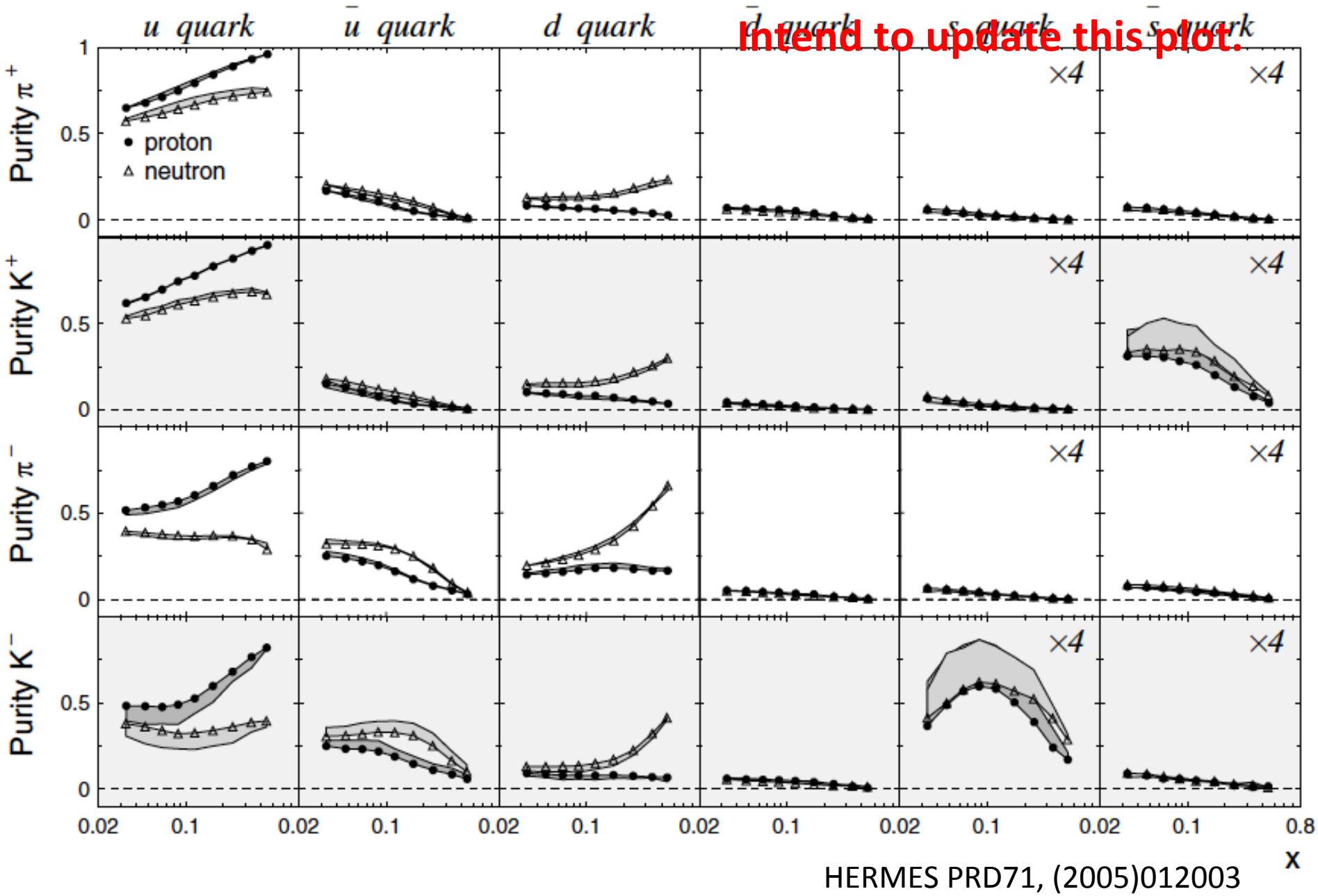

HERMES PRD71, (2005)012003

FIG. 18. Purities for positive and negative pions and kaons on a proton and a free neutron target. Each column corresponds to scattering off a certain quark flavor. The shaded bands indicate the estimated systematic uncertainties due to the fragmentation parameters. The estimate is derived from a comparison of two parameter sets. See text for details.

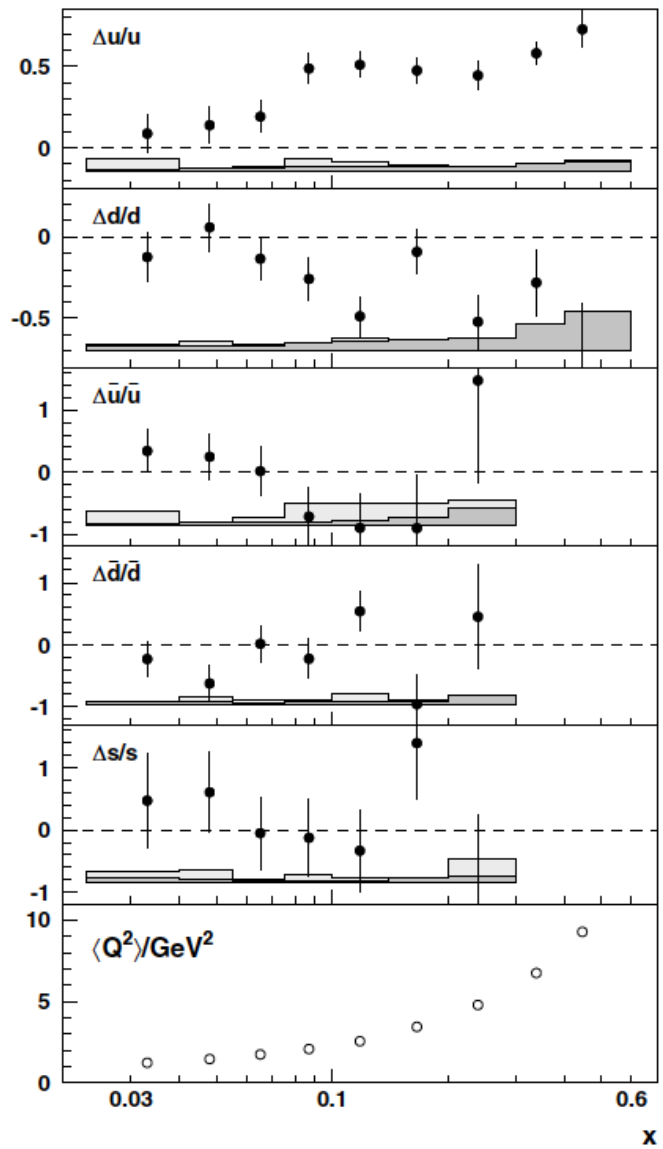

FIG. 19. The quark polarizations in the 5 parameter × 9 x-bins fit. The polarizations, shown as a function of x, were computed from the HERMES inclusive and semi-inclusive asymmetries. The error bars are the statistical uncertainties. The band represents the total systematic uncertainty, where the light gray area is the systematic error due to the uncertainties in the fragmentation model, and the dark gray area is from the contribution of the Born asymmetries.

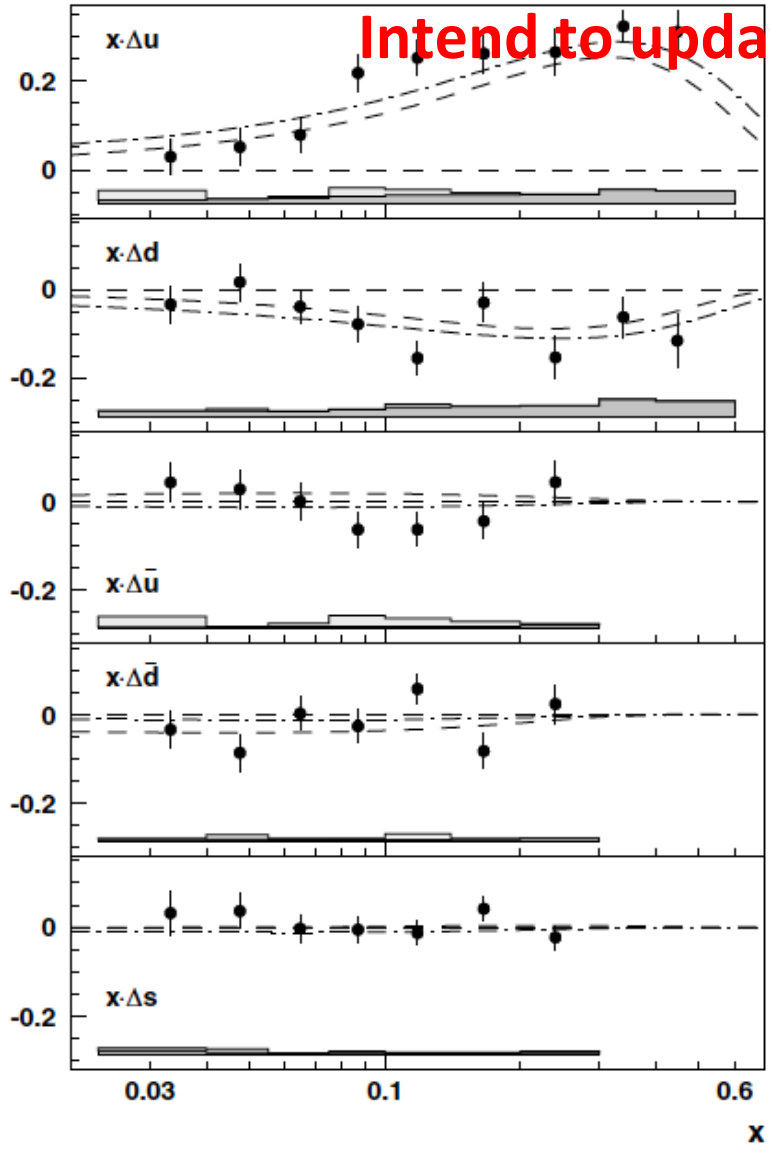

Intend to update this plot.

FIG. 20. The quark helicity distributions $x\Delta q(x, Q_0^2)$ evaluated at a common value of $Q_0^2 = 2.5\ \mathrm{GeV}^2$ as a function of x. The dashed line is the GRSV2000 parametrization (LO, valence scenario) [18] scaled with $1/(1+R)$ and the dash-dotted line is the Blümlein-Böttcher (BB) parametrization (LO, scenario 1) [67]. See Fig. 19 for explanations of the uncertainties shown.

HERMES PRD71, (2005)012003

Fragmentation Functions: DSS-2008 Assumed

SU(2), SU(3) breaking: $D_{d+\bar{d}}^{\pi^+} = N D_{u+\bar{u}}^{\pi^+}$ $\quad D_s^{\pi^+} = D_{\bar{s}}^{\pi^+} = N' D_{\bar{u}}^{\pi^+}$

but we have to assume $D_{\bar{u}}^{\pi^+} = D_d^{\pi^+}$

$$D_{\bar{u}}^{K^+} = D_s^{K^+} = D_d^{K^+} = D_{\bar{d}}^{K^+}$$

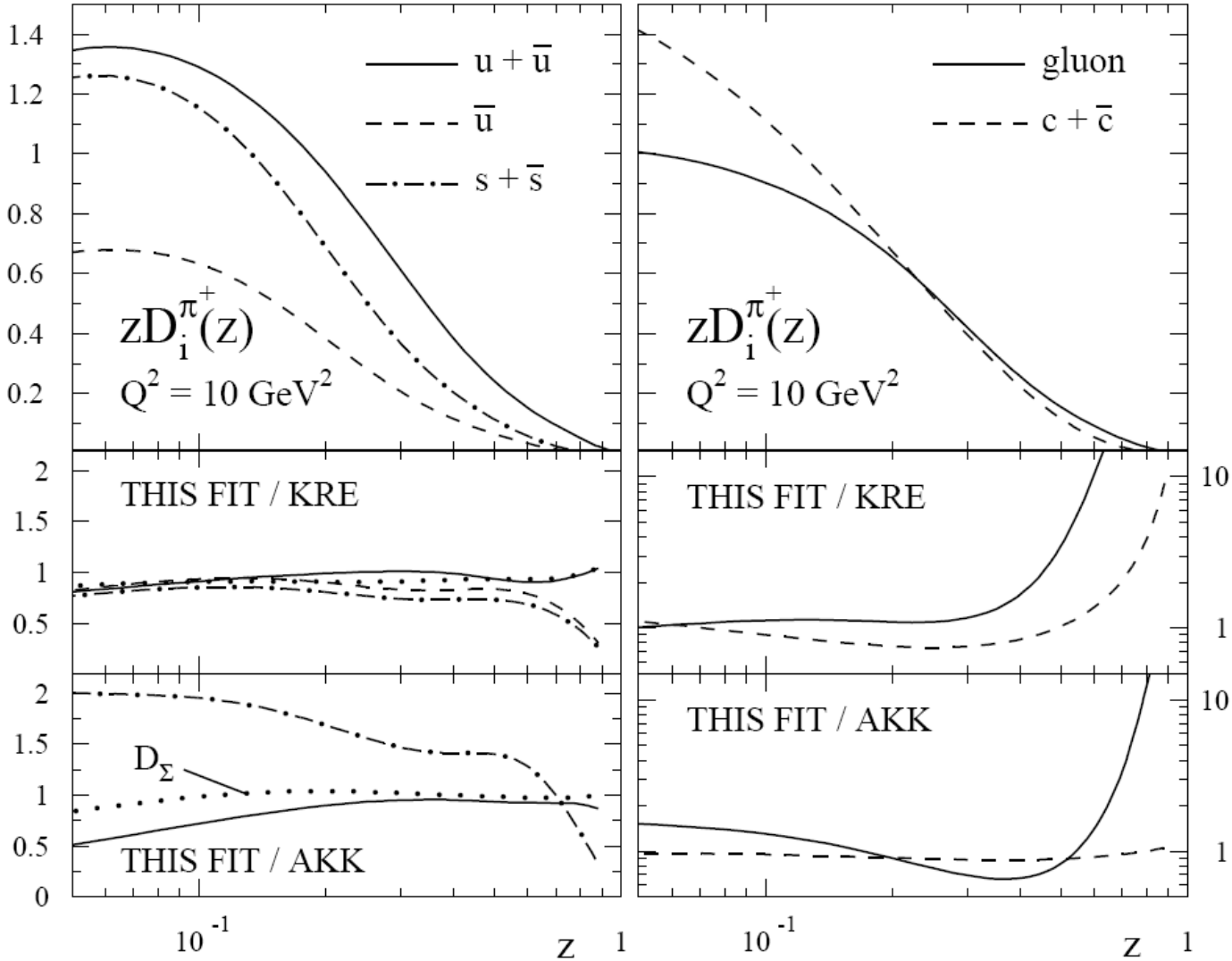

DSS-2008 Fragmentation Functions in the code
double-checked with this plot, including charm-related F.F.

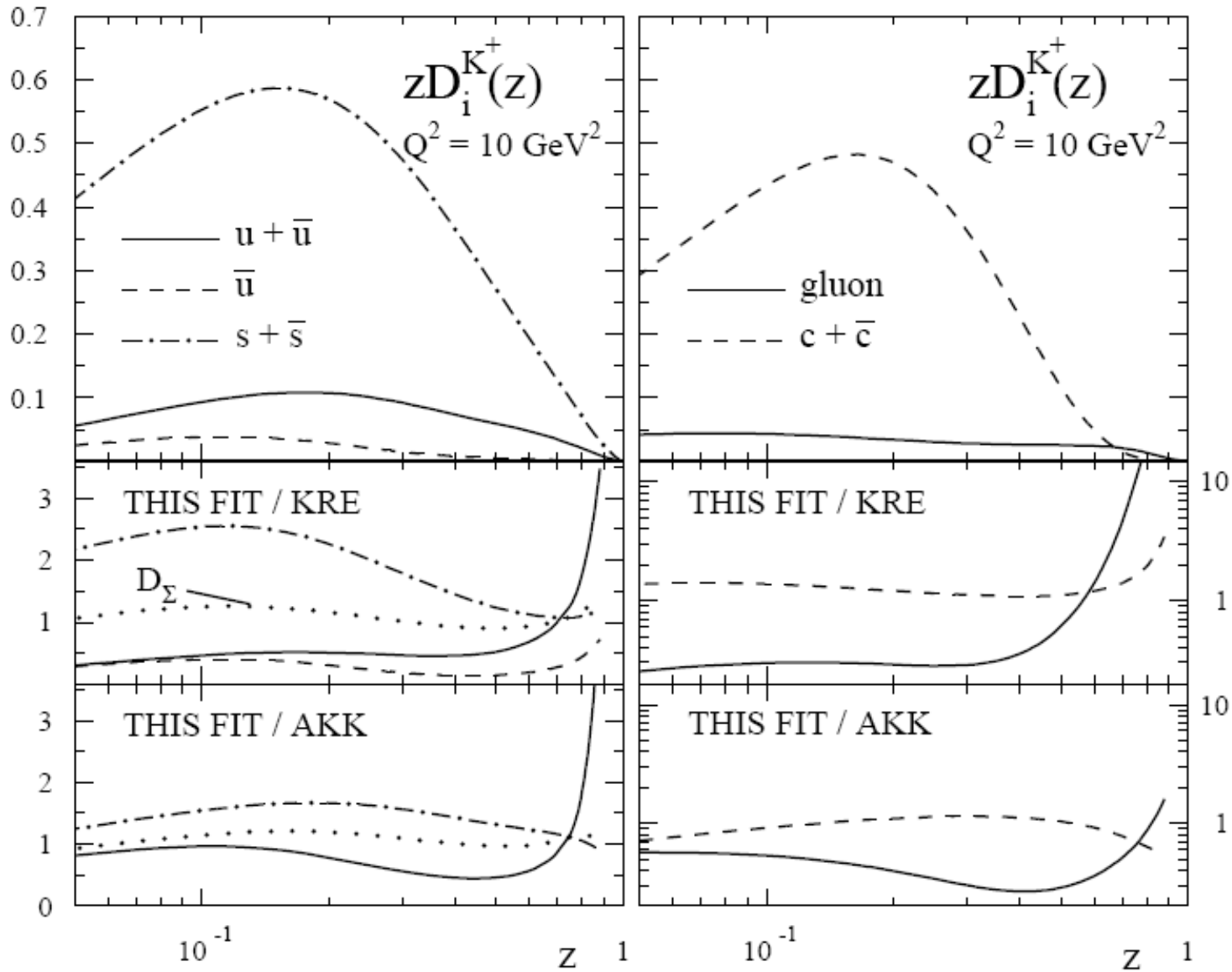

DSS-2008 Fragmentation Functions in the code
double-checked with this plot, including charm-related F.F.